

The role of IDH1 mutation on gene expression in glioblastoma

Sajad Najafi^a, Sajjad Esmaeili^b, Hossein Zhaleh^c, Yazdan Rahmati^{d,*}

^a Student Research Committee, Department of Medical Biotechnology, School of Advanced Technologies in Medicine, Shahid Beheshti University of Medical Sciences, Tehran, Iran

^b Medical Biology Research Center, Health Technology Institute, Kermanshah University of Medical Sciences, Kermanshah, Iran

^c Substance Abuse Prevention Research Center, Health Institute, Kermanshah University of Medical Sciences, Kermanshah, Iran

^d Clinical Research Development Center, Imam Khomeini and Mohammad Kermanshahi and Farabi Hospitals, Kermanshah University of Medical Sciences, Kermanshah, Iran

ARTICLE INFO

Keywords:

Glioblastoma
IDH1 mutation
TCGA
GEO
WGCNA
Meta-DE
Hub genes

ABSTRACT

Glioblastoma multiforme (GBM) is the most malignant primary brain tumor found in humans. Mutations in isocitrate dehydrogenases 1 (IDH1^{R132H}) was observed in GBM. GBMs with IDH1^{R132H} have longer patient survival compared to GBMs with wild-type IDH1 and identifying the mechanism of this can contribute to the development of a new treatment for GBM. To investigate the role of IDH1^{R132H} on gene expression, we incorporated three expression arrays from GEO including GSE36245, GSE131837, and GSE122586, and one expression array from TCGA which in total investigate gene expression differences between 293 wild type and 41 mutant IDH1 GBM samples. Meta-DE package in R software was applied to screen the differentially expressed genes (DEGs) between IDH1 wild type and IDH1^{R132H} GBMs. DEGs were used to construct co-expression networks by WGCNA package for TCGA data and genes of the detected module were used to build protein-protein interaction (PPI) network. Each of the mentioned expression arrays was analyzed independently using limma package by cutoff $|\log_{2}FC| > 1$ and $P.value < 0.05$, and 13 downregulated and 26 upregulated common genes were identified. By merging the results of limma package and core genes of the PPI network, 10 hub genes including ARAP3, ARHGAP11B, BDNF, CFAP45, CXCL8, MMP9, RHOBTB1, SHH, SYNJ2, and VEGFA were identified. Based on the TCGA database, we tested the prognostic significance of the detected genes using Kaplan-Meier survival analysis. In conclusion, the results suggested that the hub genes may play role in GBM pathogeny.

1. Introduction

According to the WHO classification, gliomas are classified into four grades in terms of histopathologic features. Glioblastoma (GBM) is in grade IV of this classification and accounts for about seventy percent of glioma malignancies. Glioblastoma is the most common and malignant primary brain tumor that has a poor prognosis despite treatment (surgery, radiotherapy, chemotherapy) and has a median survival of 12–15 months. The glioblastoma is divided into two primary and secondary subtypes. Over ninety percent of glioblastomas are of the primary type, which rapidly develops and affects older people. A secondary form of low-grade astrocytoma develops gradually into glioblastoma and affects younger people [1–3]. In the last decade, the mechanism of glioblastoma was extensively researched which led to the identification of several molecular abnormalities like IDH1^{R132H}. IDH1 catalyzes the oxidative carboxylation of isocitrate to alpha-ketoglutarate and the reduction of

NADP to NADPH that is necessary for cellular antioxidant reaction. The IDH1^{R132H} gains oncogenic function and converts alpha-ketoglutarate to the oncometabolite 2-hydroxyglutarate (2-HG) that subsequently cause genome-wide methylation change in glioblastoma patients and finally aberrant gene expression. The mutation of IDH1 is also considered a strong GBM prognostic factor [4]. The 2016 World Health Organization (WHO) Classification of Tumors of the Central Nervous System has subclassified GBM into IDH-wildtype GBM and IDH-mutant GBM [5].

In glioblastoma, the IDH1^{R132H} occurs at the active site of the enzyme and at the highly conserved codon 132 and causes Arg to His substitution. The IDH1^{R132H} has been observed in more than 95% of secondary GBMs and less than 10% of primary GBMs and is now considered a definitive marker of secondary GBMs [6]. The prognosis of GBM patients with IDH1^{R132H} is better than those with normal IDH1. GBM patients with normal IDH1 have a median survival of 15 months, but surprisingly, the median survival of GBM patients with IDH1^{R132H} is

* Corresponding author. Department of Medical Genetics, Iran University of Medical Sciences, Crossroads of Shahid Hemmat & Shahid Chamran Highways, Iran.
E-mail addresses: sajadnajafi1990@yahoo.com (S. Najafi), yazdanrahmati68@gmail.com (Y. Rahmati).

about 31 months. Clarifying the reason for better prognosis of GBM patients with IDH1^{R132H} can lead to the development new treatment strategy for gliomas [7].

To determine the effect of IDH1^{R132H} on gene expression in GBM patients, we collected raw data of 334 GBM samples from TCGA and GEO. After meta-analysis through Meta-DE package, 1054 genes were selected for the rest of analysis. By WGCNA package, we performed weighted co-expression analysis, and detected module was used for enrichment analysis and protein-protein Interaction network (PPI) construction. Using limma package, differentially expressed genes (DEGs) were detected, and by merging the results of limma package with core genes of PPI, hub genes were detected. Using survival plot the prognosis of hub genes was evaluated.

2. Methods

2.1. Gene expression profiles data

Three expression arrays including GSE36245, GSE131837, and GSE122586 from GEO (<https://www.ncbi.nlm.nih.gov/geo/>) and a dataset from TCGA (The Cancer Genome Atlas) were downloaded [8]. The selected datasets in total evaluate the expression status of 334 GBM of which 293 had normal IDH1 and 41 had mutant IDH1 (IDH1^{R132H}).

2.2. Data processing

Through quantile normalization method in limma package [9] and log₂ transformation of expression matrixes, all datasets were normalized. For better results, we included an only single measure for each gene, by the aggregate function in S4Vectors package, which gives an average measure of the probes for each gene.

2.3. Meta-analysis using Meta-DE package

Using Meta-DE package [10] differentially expressed genes were discovered. We used p-value < 0.05 and FDR < 0.05 as cutoff and moderate T-test for combination of results.

2.4. Enrichment of DEGs through Meta-Path package

By implementation of three frameworks of Meta-Path package [10] including MAPE_G (Meta-analyses for pathway enrichment at the gene level), MAPE_P (Meta-analyses for pathway enrichment at the pathway level), and MAPE_I (Meta-analyses for pathway enrichment at hybrid level) the most important signaling pathways based on p-value < 0.05 were detected.

2.5. Weighted co-expression network analysis

Using WGCNA package [11], weighted gene co-expression network of genes was constructed that includes three steps. First, sample clustering of selected genes resulted from Meta-DE. Second, choosing an appropriate soft threshold power with standard scale-free networks. Third, calculation of adjacency by pickSoftThreshold function and conversion of adjacency results into topological overlap matrix (TOM) and the corresponding dissimilarity (1-TOM). To construct the network, a minimum module size of 30, and the module detection sensitivity deep Split 2 in blockwiseConsensusModules function were adopted. The correlation between, and association of individual genes and clinical data were evaluated through defining Gene Significance (GS) as the absolute value. For each module, a quantitative criterion of module membership (MM) was taken into account as the correlation between the eigengene module and gene expression profile through which the similarity of all genes on the array datasets to every module was measured and determined. Using GS and MM, it is feasible to identify interesting module (s) containing the genes with the great significance of

both clinical data and module membership.

2.6. Protein-protein interaction (PPI) network construction

We constructed the PPI of the selected module using STRING and cytoscape [12]. ClueGO v2.5.3 [13] was utilized to perform pathway enrichment analysis of the genes, and the most important signaling pathways based upon KEGG database were detected [14].

2.7. DEGs screening

To select hub genes, each of the expression arrays was analyzed independently. We used limma package for detection of DEGs between wild type and IDH1^{R132H} GBM samples using cutoff $|\log_{2}FC| \geq 1$ and p-value < 0.05. By merging DEGs and core genes of PPI network, hub genes were selected.

2.8. Hub genes validation

Kaplan-Meier survival curve of overall survival and disease-free survival was plotted to analyze the survival differences [15].

3. Results

3.1. Meta-analysis using Meta-DE package

Four microarrays in total (GSE122586, GSE131837, GSE36245, and TCGA data) were incorporated into the analysis, which includes 334 GBM samples of which 293 with IDH1 wild and 41 with IDH1^{R132H} genes. The result of Meta-DE package was plotted as a heatmap (Fig. 1A). Using FDR < 0.01 and P.value < 0.05, 1054 genes were identified.

3.2. Enrichment of DE-genes using meta-path package

Using Meta-path package, 17 dysregulated signaling pathways were identified and plotted as a heatmap (Fig. 1B). FDR < 0.05 and P.value < 0.05 were implemented as a cutoff and signaling pathways like extracellular matrix organization, collagen formation, cell cycle, mitotic_m_g1 phases, and DNA replication based on Reactome database, focal adhesion, and ECM-receptor interaction based on KEGG database, mitotic nuclear division, and mitotic M phase based on Gene Ontology were identified.

3.3. Weighted co-expression network analysis

The results of Meta-DE package were considered as input for network construction in WGCNA package. 1054 genes and 150 GBM samples from TCGA database including 141 samples with wild type IDH1 and 8 samples with IDH1^{R132H} were used for rest of analysis (Fig. 2A). After normalization and quality assessment of expression matrix of TCGA dataset, power 7 was selected to reach scale-free network. Through hierarchical clustering for TCGA data, we detected 12 differently colored modules regarding the number of genes, and genes that could not be included in any particular module were put into the grey module (Fig. 2B and C). We selected green module (P. value = 0.0063) as main module and its scatterplot is provided (Fig. 2D).

3.4. Protein-protein interaction (PPI) network construction

135 genes of green module were used for PPI network construction in STRING database and based on the degree > 25, and betweenness centrality > 0.1 as a cutoff was visualized in Cytoscape (Fig. 3A). We enriched these genes and analyzed them through the Cytoscape plug-in ClueGo based upon KEGG database, proteoglycans in cancer, age-rage signaling pathway in diabetic complications, ECM receptor

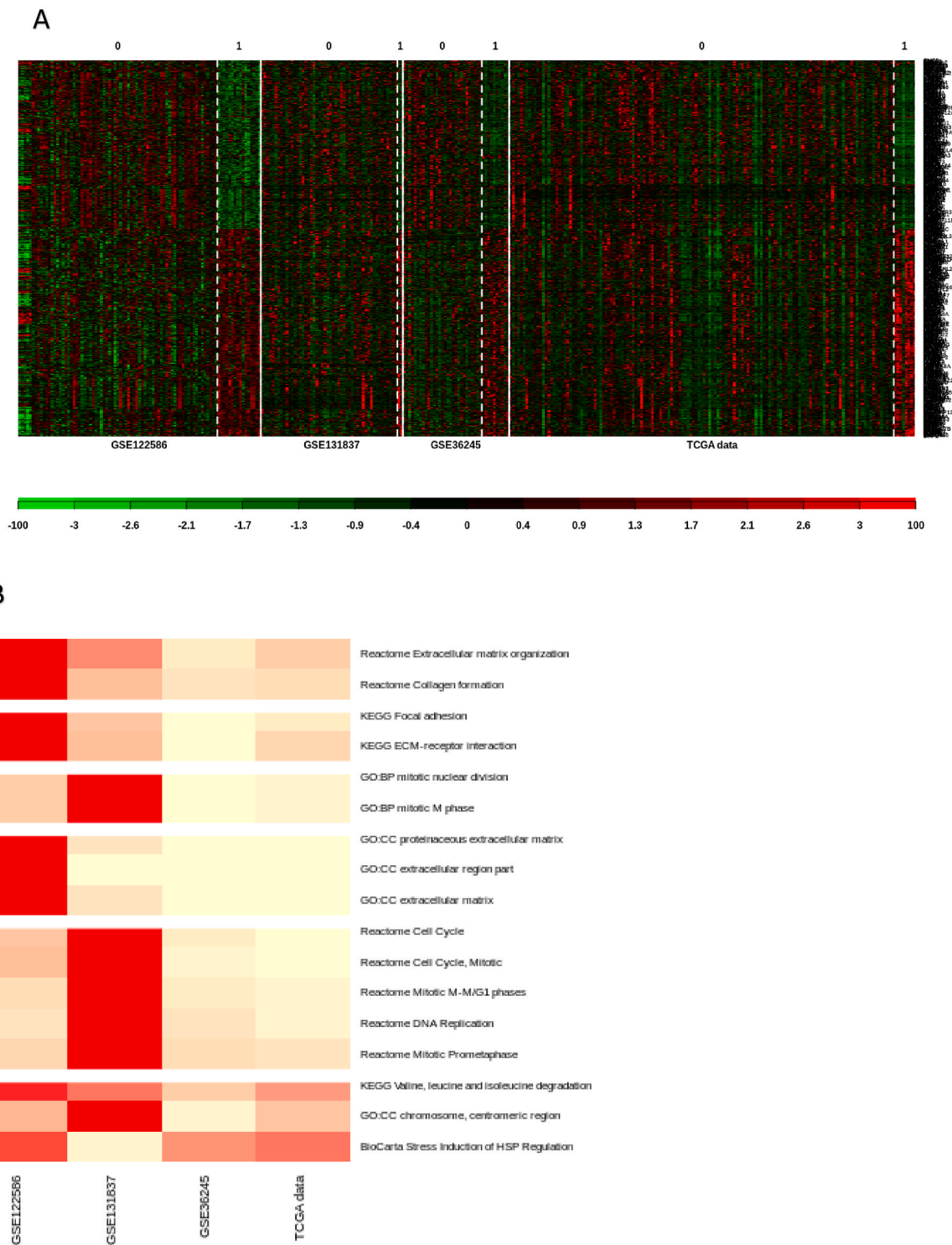


Fig. 1. (A) Hierarchical clustering heat map of 1054 DEGs from Wild type IDH1 and IDH1^{R132H} GBM samples, Red and green indicate high and low expression genes, respectively. O represent wild type IDH1 and 1 represent IDH1^{R132H} samples. (B) heatmap signaling pathways of 1054 DEGs between Wild type IDH1 and IDH1^{R132H} GBM samples differentially expressed genes between control-patients samples.

interaction, protein digestion and absorption, gap junctions, and p53 signalling pathway are the most important signaling pathways (Fig. 3B).

3.5. DEGs screening

We analyzed four expression arrays (GSE36245, GSE131837, GSE122586, and TCGA) to evaluate the gene expression level between wild type and IDH1^{R132H} GBM samples using Limma package. We

screened all the DEGs using $|\log_2FC| > 1$ and $p\text{-value} < 0.05$ as the threshold and showed them as volcano plots (Fig. 4A–D). Following overlapping, we identified 26 upregulated and 13 downregulated common genes (Fig. 4E and F). By merging the results of limma package and core genes of PPI network, ten genes including ARAP3, ARHGAP11B, BDNF, CFAP45, CXCL8, MMP9, RHOBTB1, SHH, SYNJ2, and VEGFA were selected.

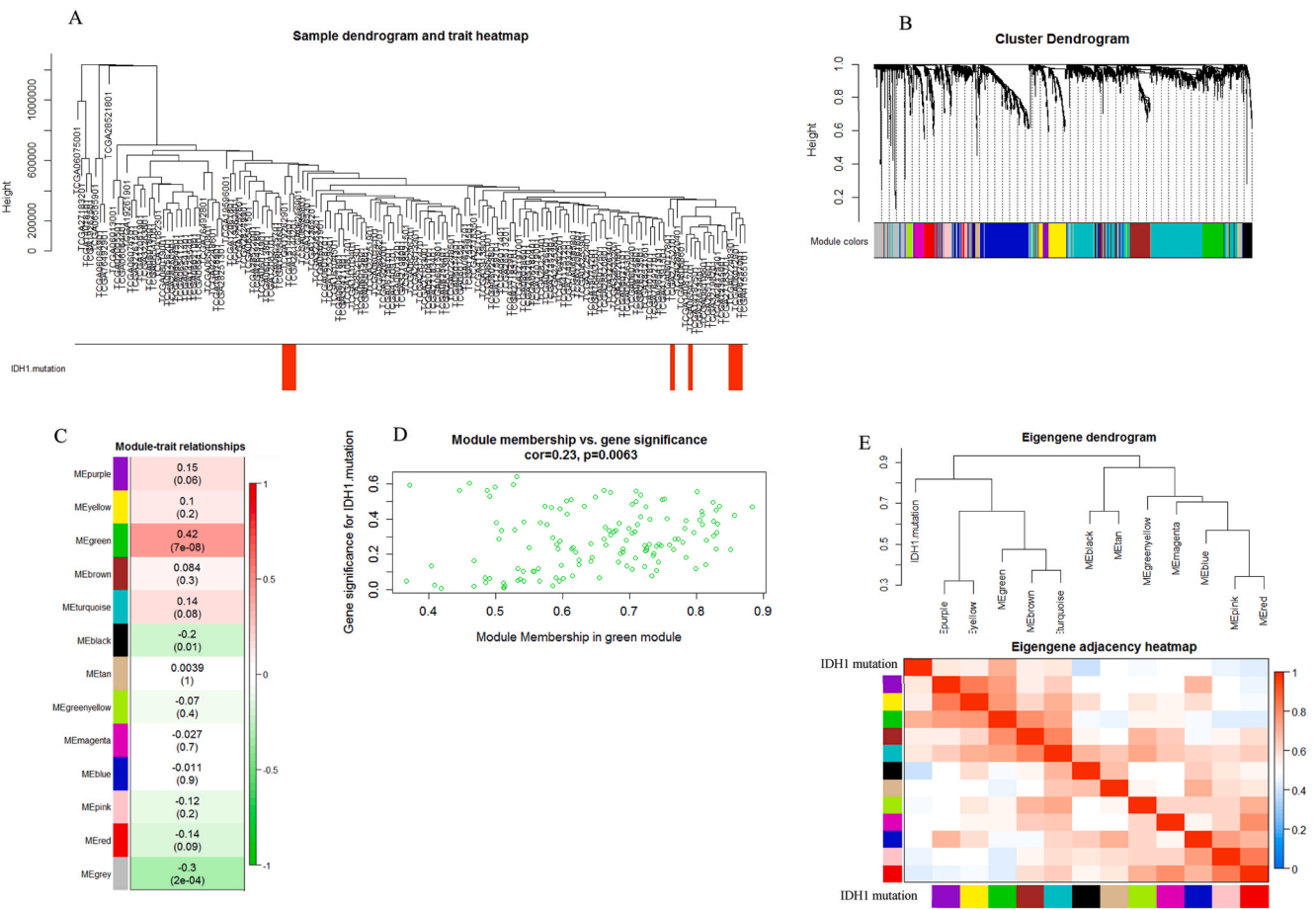


Fig. 2. WGCNA data for TCGA data. (A) Clustering dendrogram of samples based on their Euclidean distance and how the clinical traits relate to the sample dendrogram, white means IDH1 wild type, red means IDH1^{R132H} GBM samples. (B) Clustering dendrogram of DEGs with dissimilarity based on topological overlap, together with assigned module colors. Each color represents a module in the constructed gene co-expression network. (C) Module-trait associations for DEGs. Each row corresponds to a module eigengene, column to a trait. Each cell contains the corresponding correlation and p-value. The table is color-coded by correlation according to the color legend. (D) Scatterplot of Gene Significance (GS) for disease gene significance vs. Module Membership (MM) of green module. (E) Visualization of the eigengene network representing the relationships among the modules and the clinical trait disease status including hierarchical clustering dendrogram and the heatmap.

4. Discussion

Glioblastoma is the most common central nervous system tumor that initiates in brain tissue and originates from astrocyte cells [16]. The subtypes of GBM have been identified based on expression changes of some genes including TP53 (p53), epidermal growth factor receptor (EGFR), and IDH1 [17–19]. IDH1^{R132H} are significantly detectable in glioblastomas. In general, the present rate of IDH1^{R132H} is about 70%–80% [20–22]. Due to the high prevalence of IDH1^{R132H} in the GBM population, previous studies have suggested that IDH1 can be used as a biomarker for glioblastoma. The role of IDH1^{R132H}-induced tumorigenicity in glioblastomas is still under intensive investigation [22–24].

By performing meta-analysis between IDH1 wild type and IDH1^{R132H} GBM samples using Meta-DE package, we identified 1054 genes. The input data for the WGCNA construction consisted of the meta-analysis-retrieved results and 149 GBM samples obtained from the TCGA database with different IDH1 status. Genes of the green module were considered for PPI network construction. Each of the expression arrays was analyzed independently and their shared genes were identified. By merging the core genes of PPI network and the results of limma package, 10 screened genes were considered as hub genes.

The 10 hub genes included ARAP3, ARHGAP11B, BDNF, CFAP45, CXCL8, MMP9, RHOBTB1, SHH, SYNJ2, and VEGFA. ARAP3 (ArfGAP with RhoGAP domain, ankyrin repeat, and PH domain 3) can be found in

the plasma membrane and serves as a PI3K effector regulating both Arf and Rho GTPases [25]. ARAP3 dysregulation has been reported in various malignancies. It causes cell proliferation in papillary thyroid carcinoma [26]. The tumorigenic role of ARAP3 through the effect on NEDD9 has been investigated. NEDD9 is the marker of epithelial-mesenchymal transition (EMT) in breast cancer [27,28].

Brain-derived neurotrophic factor (BDNF) is one of the most common neurotrophins in the mammalian brain. BDNF acts via its receptors tropomyosin receptor kinase B (TrkB) and the low affinity p75 neurotrophin receptor (p75NTR) [29]. BDNF signaling is involved in several essential processes in the brain synapses and considered as essential mediator of plasticity in the CNS [29]. BDNF overexpression has been found in many types of cancer like bladder, NSCLC, colorectal, and breast carcinomas with suggested therapeutic potentials [30–32]. In glioma cell lines, BDNF also has been shown to promote tumor cell growth and migration [33]. High expression levels of BDNF predicts tumor remission and poor prognosis and survival for the cancerous patients [34].

ARHGAP11B is a human-specific gene which is found to be localized in mitochondria and favorably expressed in human neural progenitors of fetal neocortex with highest expression level in radial glial cells [35]. It has been known to be evolutionarily appeared in human after separation from chimpanzee by partial duplication of ARHGAP11A gene which encodes a Rho GTPase activating protein (Rho-GAP). ARHGAP11B may

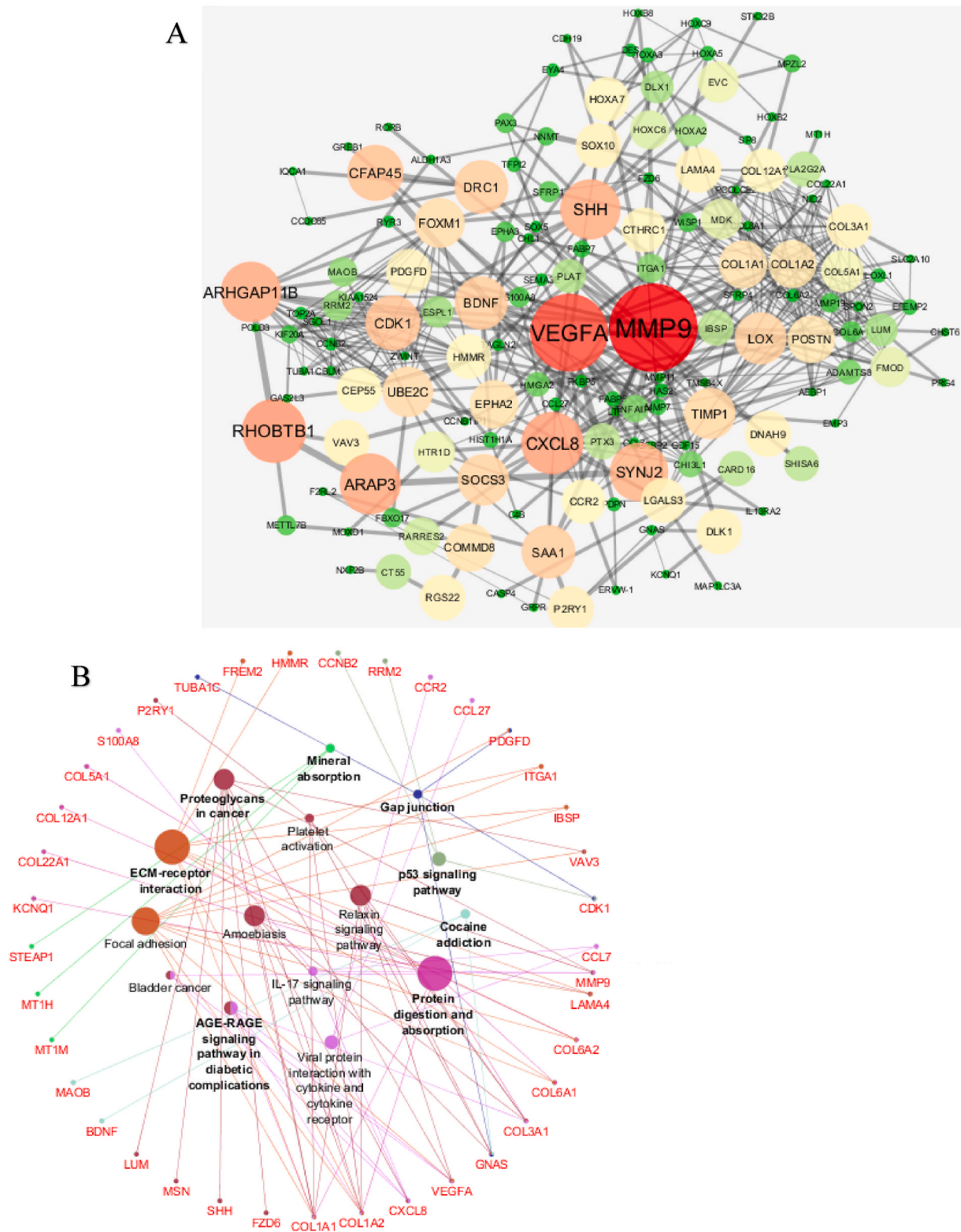


Fig. 3. (A) Protein-protein interaction network of the DEGs. Showing genes with the highest number of interactions. The gradual change in the size indicates the connectivity degree. The gradual change in the color indicates the betweenness centrality. The thickness of the edges stands for the credibility. (B) Enriched KEGG pathways using the ClueGo plugin of Cytoscape. Functionally grouped networks based on KEGG database of Genes with terms as nodes linked based on their κ score level.

act as a contributor to neocortex expansion in humans by increasing its size and folding and enhances the generation of basal progenitors and self-renewal in mice [36]. ARHGAP11A protein is suggested to play role in multiple cancers including glioblastoma [37], however ARHGAP11B

requires further studies to reveal its potential role in tumorigenesis although it is known that ARHGAP11B enhances basal progenitor cell proliferation.

Cilia and flagella associated protein 45 (CFAP45) gene (also known as

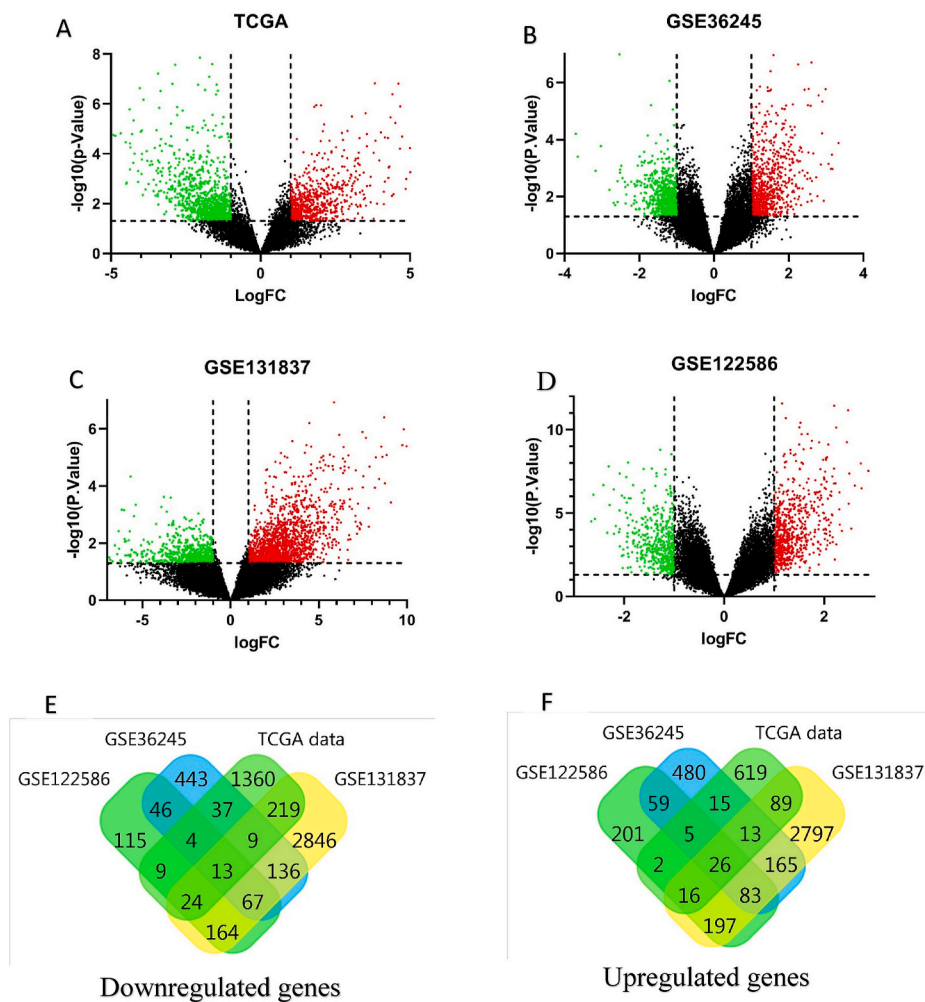


Fig. 4. Differentially expressed genes and common differentially expressed genes in four datasets between IDH1 wild type and IDH1^{R132H} GBM samples. (A, B, C, D) The volcano plots of differentially expressed genes in TCGA data, GSE36245, GSE131837, and GSE122586 respectively using P.Value < 0.05 and |log2fold change| ≥ 1. (E, F) Common differentially expressed genes in four datasets.

NESG1 and *CCDC19*) encodes the CFAP45 protein which is preferentially expressed in human nasopharynx, trachea, and sperm flagella where stroke power and motility, respectively are associated physiological activities. CFAP45 deficiency has been revealed to cause situs abnormalities and asthenospermia [38], more importantly CFAP45 acts as a tumor suppressor preventing tumor cell proliferation, invasion, and metastasis [39] and thus its downregulation is especially associated with nasopharyngeal carcinoma (NPC) and NSCLC [40].

CXC Chemokine Ligand 8 or *CXCL8 (Interleukin-8, IL-8)* gene encodes IL-8 which is secreted from many blood cells in response to infections, hypoxic conditions and more importantly found to be involved in tumorigenesis [41]. CXCL8 protein plays a critical role in inflammation-mediated tissue damage and its upregulation is associated with diseases of the central nervous system (CNS) like multiple sclerosis [41]. Additionally, CXCL8 has been found to show mitogenic effects and so expressed on cell membrane of cancer cells along with its receptors CXCR1 and 2 form an axis stimulating cancer growth [42,43]. Similarly, in glioblastoma cells CXCL8 has been shown to be upregulated [44], enhances progression of glioma via activating the JAK/STAT1/HIF-1 α /Snail signaling pathway [45] and its high expression predicts recurrence of glioblastoma [46].

Matrix metalloproteinase 9 (MMP9) gene encodes the MMP9 protein which is a zinc-dependent endopeptidase, produced in inactive “pro” form and requires NH₂-terminal enzymatic digestion to be activated [47]. Same to other metalloproteases, MMP9 facilitates tumor

progression by enhancement in tumor cell proliferation, migration, invasion, and particularly metastasis via affecting extracellular matrix (ECM) [47]. In consistent with studies on other types of cancer, in glioblastoma cell lines, MMP9 has been found to be significantly increased via enhanced gene copy numbers compared with normal controls, promotes cell growth and tumorigenesis, also its expression levels are associated with clinical grades of the disease [48,49].

Rho-related BTB domain containing 1 (RHOBTB1) is a tumor suppressor gene located on chromosome 10q21.3 encodes a protein which belongs to a subfamily of Rho GTPase family. Proteins of this subfamily are atypical GTPases which are larger related to conventional Rho GTPases, containing extra domains and unlike others don't turn between GTP- and GDP-bounded forms [50]. *RHOBTB1* and 3 play roles in cell membrane trafficking events and cytoskeletal organization [51]. *RHOBTB1* was first suggested as a tumor suppressor in head and neck cancer [52], now studied in many other cancers and its depletion is associated with increased tumorigenesis [50]. *RHOBTB1* mutations have been identified as one of the driving genetic causes in glioblastoma [53].

Sonic hedgehog (*SHH*) gene is member of a family which have been conserved among vertebrate during evolution. *SHH* is expressed in many various tissues including CNS during early human development involved in especially anterior-posterior limb axis and specification of different cells in brain and neural tube [54,55]. *SHH* acts as the ligand in the Hedgehog signaling pathway which its dysregulation has been associated with anomalies and several sporadic cancers such as

medulloblastoma, colon, pancreatic metastases, small cell lung carcinomas, and cancer stem cells (CSCs) of glioma [56,57].

SYNJ2 gene encodes Synaptojanin 2 polyphosphoinositide phosphatase which plays role as an effector for Rac1 GTPase of the Rho GTPases family [58], regulates clathrin-mediated endocytosis and thus mediates Rac1 control over cell growth control [59]. Synaptojanin 2 dysregulation or some polymorphisms are established to contribute to several cancers such as colorectal, breast, and glioma tumorigenesis [58, 60] and its depletion inhibited lamellipodia and invadopodia formation, and prevented migration and invasion of glioblastoma cell lines [61].

VEGFA gene encodes for vascular endothelial growth factor A produced by endothelial cells, infiltrating myeloid cells and hypoxic tumor cells contributes to expansion of a vascular bed for cancer cells [62]. *VEGFA* via interaction with its receptors especially *VEGFR 2* activates several signaling pathways *PI3K/Akt* and *Rho GTPases* plays an important role in regulation of angiogenesis, vascular permeability, and inflammation [62]. Dysregulation of *VEGFA* has been linked with enhanced tumorigenesis in a wide variety of cancers. Similarly, glioblastoma cell lines have been found to secrete *VEGFA* in extracellular vesicles [63], positively influences glioblastoma development in model cells [64], and causes increased invasive factor *MMP2* to facilitate progression [63].

Taken together, these 10 genes as the hub genes, which we identified to change on *IDH1* expression in GBM, are previously known to play role in various cellular functions. Among them, several are particularly involved in development and progression of human cancers. Thus, we suggest that *IDH1* mutation may affect gene expression pattern in GBM, which in turn potentially can promote progression and aggressiveness of the malignancy. This assertion requires particularly experimental investigations to be validated.

5. Conclusion

This study is among the first attempts evaluating the effect of *IDH1R132H* mutation compared to *IDH1* wild type on the whole-genome expression in GBM samples. In total 334 GBM samples including 293 wild type and 41 *IDH1R132H* from both TCGA and GEO databases were incorporated into the study. Meta-DE package was used for meta-analysis and WGCNA was employed to construct the co-expression networks. PPI network of the detected module was built using STRING and Cytoscape. Finally, 10 hub genes including *ARAP3*, *ARHGAP11B*, *BDNF*, *CFAP45*, *CXCL8*, *MMP9*, *RHOBTB1*, *SHH*, *SYNJ2*, and *VEGFA* were detected, which their expression was approved by analyzing each of the expression arrays independently. The prognostic potentials of the hub genes were validated by plotting the Kaplan-Meier survival curve. Based on the previously identified roles of these genes in literature, they are suggested that may be involved in cellular processes, which can lead to promoted aggressiveness of GBM. Further investigations are recommended to explore the precise roles of these genes in GBM pathogeny.

Declaration of competing interest

The authors declare that they have no known competing financial interests or personal relationships that could have appeared to influence the work reported in this paper.

Acknowledgement

This study was funded by Kermanshah University of medical sciences.

References

[1] Cohen AL, Colman H. Ricky Chen, Matthew Smith-Cohn.

- [2] Hill VK, Shinawi T, Ricketts CJ, Krex D, Schackert G, Bauer J, et al. Stability of the CpG island methylator phenotype during glioma progression and identification of methylated loci in secondary glioblastomas 2014;14(1):506.
- [3] Smith AA, Huang Y-T, Eliot M, Houseman EA, Marsit CJ, Wiencke JK, et al. A novel approach to the discovery of survival biomarkers in glioblastoma using a joint analysis of DNA methylation and gene expression 2014;9(6):873–83.
- [4] Polivka Jr J, Pesta M, Pitule P, Hes O, Holubec L, Polivka J, et al. *IDH1* mutation is associated with lower expression of VEGF but not microvessel formation in glioblastoma multiforme. *Oncotarget* 2018;9(23):16462.
- [5] Zhang M, Ye G, Li J, Wang Y. Recent advance in molecular angiogenesis in glioblastoma: the challenge and hope for anti-angiogenic therapy. *Brain Tumor Pathol* 2015;32(4):229–36.
- [6] Dang L, Yen K, Attar EJAoO. *IDH* mutations in cancer and progress toward development of targeted therapeutics 2016;27(4):599–608.
- [7] Miyata S, Tominaga K, Sakashita E, Urabe M, Onuki Y, Gomi A, et al. Comprehensive metabolomic analysis of *IDH1 R132H* clinical glioma samples reveals suppression of β -oxidation due to carnitine deficiency. *Sci Rep* 2019;9(1): 1–11.
- [8] Brennan CW, Verhaak RG, McKenna A, Campos B, Nounshmehr H, Salama SR, et al. The somatic genomic landscape of glioblastoma. *Cell* 2013;155(2):462–77.
- [9] Smyth GK. Limma: linear models for microarray data. In: *Bioinformatics and computational biology solutions using R and Bioconductor*. Springer; 2005. p. 397–420.
- [10] Wang X, Kang DD, Shen K, Song C, Lu S, Chang L-C, et al. An R package suite for microarray meta-analysis in quality control, differentially expressed gene analysis and pathway enrichment detection. *Bioinformatics* 2012;28(19):2534–6.
- [11] Langfelder P, Horvath S. WGCNA: an R package for weighted correlation network analysis. *BMC Bioinf* 2008;9(1):559.
- [12] Shannon P, Markiel A, Ozier O, Baliga NS, Wang JT, Ramage D, et al. Cytoscape: a software environment for integrated models of biomolecular interaction networks. *Genome Res* 2003;13(11):2498–504.
- [13] Bindea G, Mlecnik B, Hackl H, Charoentong P, Tosolini M, Kirilovsky A, et al. ClueGO: a Cytoscape plug-in to decipher functionally grouped gene ontology and pathway annotation networks. *Bioinformatics* 2009;25(8):1091–3.
- [14] Kanehisa M, Araki M, Goto S, Hattori M, Hirakawa M, Itoh M, et al. KEGG for linking genomes to life and the environment. *Nucleic Acids Res* 2007;36(suppl_1): D480–4.
- [15] Gao J, Aksoy BA, Dogrusoz U, Dresdner G, Gross B, Sumer SO, et al. Integrative analysis of complex cancer genomics and clinical profiles using the cBioPortal. *Sci Signal* 2013;6(269):p11–.
- [16] Bleeker FE, Molenaar RJ, Leenstra S. Recent advances in the molecular understanding of glioblastoma. *J Neuro-oncol* 2012;108(1):11–27.
- [17] Verhaak RG, Hoadley KA, Purdom E, Wang V, Qi Y, Wilkerson MD, et al. Integrated genomic analysis identifies clinically relevant subtypes of glioblastoma characterized by abnormalities in *PDGFRA*, *IDH1*, *EGFR*, and *NF1*. *Cancer Cell* 2010;17(1):98–110.
- [18] Bleeker FE, Lamba S, Zanon C, Molenaar RJ, Hulsebos TJ, Troost D, et al. Mutational profiling of kinases in glioblastoma. *BMC Cancer* 2014;14(1):718.
- [19] Hayden EC. Genomics boosts brain-cancer work. *Nature Publishing Group*; 2010.
- [20] Sanson M, Marie Y, Paris S, Idhahh A, Laffaire J, Ducray F, et al. Isocitrate dehydrogenase 1 codon 132 mutation is an important prognostic biomarker in gliomas. *J Clin Oncol* 2009;27(25):4150–4.
- [21] Håvik AB, Brandal P, Honne H, Dahlback H-S, Scheie D, Hektoen M, et al. MGMT promoter methylation in gliomas-assessment by pyrosequencing and quantitative methylation-specific PCR. *J Transl Med* 2012;10(1):36.
- [22] Nobusawa S, Watanabe T, Kleihues P, Ohgaki H. *IDH1* mutations as molecular signature and predictive factor of secondary glioblastomas. *Clin Cancer Res* 2009; 15(19):6002–7.
- [23] Weller M, Felsberg J, Hartmann C, Berger H, Steinbach JP, Schramm J, et al. Molecular predictors of progression-free and overall survival in patients with newly diagnosed glioblastoma: a prospective translational study of the German Glioma Network. *J Clin Oncol* 2009;27(34):5743–50.
- [24] Hartmann C, Hentschel B, Wick W, Capper D, Felsberg J, Simon M, et al. Patients with *IDH1* wild type anaplastic astrocytomas exhibit worse prognosis than *IDH1*-mutated glioblastomas, and *IDH1* mutation status accounts for the unfavorable prognostic effect of higher age: implications for classification of gliomas. *Acta Neuropathol* 2010;120(6):707–18.
- [25] Krugmann S, Anderson K, Ridley S, Risso N, McGregor A, Coadwell J, et al. Identification of *ARAP3*, a novel *PI3K* effector regulating both *Arf* and *Rho GTPases*, by selective capture on phosphoinositide affinity matrices. *Mol Cell* 2002; 9(1):95–108.
- [26] Wang Q-X, Chen E-D, Cai Y-F, Zhou Y-L, Zheng Z-C, Wang Y-H, et al. Next-generation sequence detects *ARAP3* as a novel oncogene in papillary thyroid carcinoma. *OncoTargets Ther* 2016;9:7161.
- [27] Kong C, Wang C, Wang L, Ma M, Niu C, Sun X, et al. *NEDD9* is a positive regulator of epithelial-mesenchymal transition and promotes invasion in aggressive breast cancer. *PLoS One* 2011;6(7):e22666.
- [28] Li P, Sun T, Yuan Q, Pan G, Zhang J, Sun D. The expressions of *NEDD9* and *E-cadherin* correlate with metastasis and poor prognosis in triple-negative breast cancer patients. *OncoTargets Ther* 2016;9:5751.
- [29] Colucci-D'Amato L, Speranza L, Volpicelli F. Neurotrophic factor *BDNF*, physiological functions and therapeutic potential in depression, neurodegeneration and brain cancer. *Int J Mol Sci* 2020;21(20):7777.
- [30] Lai PC, Chiu TH, Huang YT. Overexpression of *BDNF* and *TrkB* in human bladder cancer specimens. *Oncol Rep* 2010;24(5):1265–70.

- [31] Yang X, Martin TA, Jiang WG. Biological influence of brain-derived neurotrophic factor (BDNF) on colon cancer cells. *Exp Ther Med* 2013;6(6):1475–81.
- [32] Tajbakhsh A, Mokhtari-Zaer A, Rezaee M, Afzaljavan F, Rivandi M, Hassanian SM, et al. Therapeutic potentials of BDNF/TrkB in breast cancer; current status and perspectives. *J Cell Biochem* 2017;118(9):2502–15.
- [33] Xiong J, Zhou L, Lim Y, Yang M, Zhu YH, Li ZW, et al. Mature BDNF promotes the growth of glioma cells in vitro. *Oncol Rep* 2013;30(6):2719–24.
- [34] Okamura K, Harada T, Wang S, Ijichi K, Furuyama K, Koga T, et al. Expression of TrkB and BDNF is associated with poor prognosis in non-small cell lung cancer. *Lung Cancer* 2012;78(1):100–6.
- [35] Namba T, Dóczi J, Pinson A, Xing L, Kalebic N, Wilsch-Bräuninger M, et al. Human-specific ARHGAP11B acts in mitochondria to expand neocortical progenitors by glutaminolysis. *Neuron* 2020;105(5):867–81. e9.
- [36] Florio M, Albert M, Taverna E, Namba T, Brandl H, Lewitus E, et al. Human-specific gene *ARHGAP11B* promotes basal progenitor amplification and neocortex expansion. *Science* 2015;347(6229):1465–70.
- [37] Zhou H-N, Ren Y-X, Li L, Wang K-S, Jiao Z-Y. Function of Rho GTPase activating protein 11A in tumors. *Chin Med J* 2018;131(11):1365–6.
- [38] Dougherty GW, Mizuno K, Nöthe-Menchen T, Ikawa Y, Boldt K, Ta-Shma A, et al. CFAP45 deficiency causes situs abnormalities and asthenospermia by disrupting an axonemal adenine nucleotide homeostasis module. *Nat Commun* 2020;11(1):5520.
- [39] Liu Z, Li X, He X, Jiang Q, Xie S, Yu X, et al. Decreased expression of updated NESG1 in nasopharyngeal carcinoma: its potential role and preliminarily functional mechanism. *Int J Cancer* 2011;128(11):2562–71.
- [40] Liang Z, Liu Z, Cheng C, Wang H, Deng X, Liu J, et al. VPS33B interacts with NESG1 to modulate EGFR/PI3K/AKT/c-Myc/P53/miR-133a-3p signaling and induce 5-fluorouracil sensitivity in nasopharyngeal carcinoma. *Cell Death Dis* 2019;10(4):305.
- [41] Lund BT, Ashikian N, Ta HQ, Chakrany Y, Manoukian K, Groshen S, et al. Increased CXCL8 (IL-8) expression in multiple sclerosis. *J Neuroimmunol* 2004;155(1–2):161–71.
- [42] Zhu YM, Woll PJ. Mitogenic effects of interleukin-8/CXCL8 on cancer cells. *Future Oncol* 2005;1(5):699–704.
- [43] Ha H, Debnath B, Neamati N. Role of the CXCL8-CXCR1/2 Axis in cancer and inflammatory diseases. *Theranostics* 2017;7(6):1543–88.
- [44] Gabellini C, Castellini L, Trisciuglio D, Kracht M, Zupi G, Del Bufalo D. Involvement of nuclear factor-kappa B in bcl-xL-induced interleukin 8 expression in glioblastoma. *J Neurochem* 2008;107(3):871–82.
- [45] Chen Z, Mou L, Pan Y, Feng C, Zhang J, Li J. CXCL8 promotes glioma progression by activating the JAK/STAT1/HIF-1 α /Snail signaling Axis. *OncoTargets Ther* 2019;12:8125–38.
- [46] Luo X, Xu S, Zhong Y, Tu T, Xu Y, Li X, et al. High gene expression levels of VEGFA and CXCL8 in the peritumoral brain zone are associated with the recurrence of glioblastoma: a bioinformatics analysis. *Oncol Lett* 2019;18(6):6171–9.
- [47] Belotti D, Paganoni P, Manenti L, Garofalo A, Marchini S, Taraoletti G, et al. Matrix metalloproteinases (MMP9 and MMP2) induce the release of vascular endothelial growth factor (VEGF) by Ovarian carcinoma cells. *Implic. Ascites Form.* 2003;63(17):5224–9.
- [48] Xue Q, Cao L, Chen XY, Zhao J, Gao L, Li SZ, et al. High expression of MMP9 in glioma affects cell proliferation and is associated with patient survival rates. *Oncol Lett* 2017;13(3):1325–30.
- [49] Wang R, Zhang S, Chen X, Li N, Li J, Jia R, et al. EIF4A3-induced circular RNA MMP9 (circMMP9) acts as a sponge of miR-124 and promotes glioblastoma multiforme cell tumorigenesis. *Mol Cancer* 2018;17(1):166.
- [50] Haga RB, Garg R, Collu F, Borda D'Agua B, Menéndez ST, Colomba A, et al. RhoBTB1 interacts with ROCKs and inhibits invasion. *Biochem J* 2019;476(17):2499–514.
- [51] Long M, Kranjc T, Mysior MM, Simpson JC. RNA interference screening identifies novel roles for RhoBTB1 and RhoBTB3 in membrane trafficking events in mammalian cells. *Cells* 2020;9(5):1089.
- [52] Beder LB, Gunduz M, Ouchida M, Gunduz E, Sakai A, Fukushima K, et al. Identification of a candidate tumor suppressor gene RHOBTB1 located at a novel allelic loss region 10q21 in head and neck cancer. *J Cancer Res Clin Oncol* 2006;132(1):19–27.
- [53] Yuan Y, Qi P, Xiang W, Yanhui L, Yu L, Qing M. Multi-omics analysis reveals novel subtypes and driver genes in glioblastoma. *Front Genet* 2020;11:565341.
- [54] Odent S, Attié-Bitach T, Blayau M, Mathieu M, Augé J, Delezoide AL, et al. Expression of the sonic hedgehog (SHH) gene during early human development and phenotypic expression of new mutations causing holoprosencephaly. *Hum Mol Genet* 1999;8(9):1683–9.
- [55] Ingham PW. The patched gene in development and cancer. *Curr Opin Genet Dev* 1998;8(1):88–94.
- [56] Skoda AM, Simovic D, Karin V, Kardum V, Vranic S, Serman L. The role of the Hedgehog signaling pathway in cancer: a comprehensive review. *Bosn J Basic Med Sci* 2018;18(1):8–20.
- [57] Niyaz M, Khan MS, Mudassar S. Hedgehog signaling: an achilles' heel in cancer. *Transl. Oncol.* 2019;12(10):1334–44.
- [58] Ben-Chetrit N, Chetrit D, Russell R, Körner C, Mancini M, Abdul-Hai A, et al. Synaptotagmin 2 is a druggable mediator of metastasis and the gene is overexpressed and amplified in breast cancer. *Sci Signal* 2015;8(360). ra7-ra.
- [59] Malecz N, McCabe PC, Spaargaren C, Qiu R, Chuang Y, Symons M. Synaptotagmin 2, a novel Rac1 effector that regulates clathrin-mediated endocytosis. *Curr Biol* : CB 2000;10(21):1383–6.
- [60] Du Q, Guo X, Zhang X, Zhou W, Liu Z, Wang J, et al. SYNJ2 variant Rs9365723 is associated with colorectal cancer risk in Chinese han population. *Int J Biol Markers* 2016;31(2):138–43.
- [61] Chuang Y-y, Tran NL, Rusk N, Nakada M, Berens ME, Symons M. Role of Synaptotagmin 2 in glioma cell migration and invasion. *Cancer Res* 2004;64(22):8271–5.
- [62] Claesson-Welsh L, Welsh M. VEGFA and tumour angiogenesis. *J Intern Med* 2013;273(2):114–27.
- [63] Treps L, Perret R, Edmond S, Ricard D, Gavard J. Glioblastoma stem-like cells secrete the pro-angiogenic VEGF-A factor in extracellular vesicles. *J Extracell Vesicles* 2017;6(1):1359479.
- [64] Gong J, Zhu S, Zhang Y, Wang J. Interplay of VEGFA and MMP2 regulates invasion of glioblastoma. *Tumor Biol* 2014;35(12):11879–85.